

Membrane tubulation from giant lipid vesicles in alternating electric fieldsK. Antonova,¹ V. Vitkova,¹ and C. Meyer²¹*Institute of Solid State Physics, Bulgarian Academy of Sciences, 72 Tzarigradsko chaussee, Sofia 1784, Bulgaria*²*Laboratoire de Physique des Systèmes Complexes, Université de Picardie Jules Verne, 33 rue Saint Leu, 80039 Amiens, France*

(Received 19 August 2015; revised manuscript received 30 November 2015; published 25 January 2016)

We report on the formation of tubular membrane protrusions from giant unilamellar vesicles in alternating electric fields. The construction of the experimental chamber permitted the application of external AC fields with strength of dozens of V/mm and kHz frequency during relatively long time periods (several minutes). Besides the vesicle electrodeformation from quasispherical to prolate ellipsoidal shape, the formation of long tubular membrane protrusions with length of up to several vesicle diameters, arising from the vesicular surface in the field direction, was registered and analyzed. The threshold electric field at which the electro-induced protrusions appeared was lower than the field strengths inducing membrane electroporation.

DOI: [10.1103/PhysRevE.93.012413](https://doi.org/10.1103/PhysRevE.93.012413)**I. INTRODUCTION**

The morphological and topological diversity of biological cells is closely related to the physical properties and the dynamic behavior of their membranes. Various sources of membrane shape transformations have been discussed [1–5]. The role of the lateral interactions between surface-bound proteins and the lipid molecules constituting the bilayer has been explored [6–9]. Some amphipathic molecules bound to the liposome surface were reported to generate spherical buds while other amphiphiles were found to pull up tubules [10–13]. Aqueous phase separations in solution mixtures enclosed in vesicles were also reported to induce budding [14]. Gradients of pH were studied as other sources of the vesicle morphological variety [15,16]. The influence of external electric fields on the morphology of giant unilamellar vesicles (GUVs) has been extensively explored also [17–23]. In alternating electric fields relatively weak shape deformations from sphere to ellipsoid have been reported [17,18,20,22,23]. It is now well established [18,21,22] that in the low-frequency range, the deformed vesicle shape is an elongated (prolate) ellipsoid, while at higher frequencies the vesicle becomes an oblate ellipsoid keeping the orientation of its rotational axis along the field. The prolate-oblate transition frequency is related to the vesicle size and to the conductivities of the aqueous media inside and outside the vesicle as discussed in details in Refs. [21,22]. The degree of the vesicle deformation at a given field strength has been found to depend on the membrane surface tension, lower tensions resulting in larger deformations [18]. Here we enrich this picture by reporting on the formation of tubular membrane protrusions (referred hereafter also as tethers and tubes) of prolate GUVs in an AC electric field.

II. EXPERIMENTAL**A. Vesicle preparation**

GUVs were obtained by electroformation [24] in a chamber consisting of two indium-tin oxide (ITO) -coated plates (4 × 4 cm), separated by a silicone (polydimethylsiloxane) spacer (0.5 cm thick) [25]. Polydimethylsiloxane (PDMS, Sylgard 184 silicone elastomer kit) was provided by Dow Corning GmbH (Germany). Methanol and chloroform (“for

analysis” grade) were purchased from Fluka (Germany) and used for the dissolution of the lipid 1-stearoyl-2-oleoyl-sn-glycero-3-phospho-choline (SOPC, Avanti Polar Lipids, USA). The vesicular suspensions were prepared in the manner that vesicular membranes enclose sucrose (Sigma Ultra[®], Sigma-Aldrich Chemie, Germany) solution, while the suspending medium was a solution of glucose (Merck, Germany) with concentration, ensuring iso-osmolar conditions on both sides of the vesicle membrane. Bidistilled water was used for the preparation of the sugar solutions. Their conductivity (17 μS/cm) was measured using Hydromat LM302 (Dresden, Germany). Lipid depositions were made by the spreading of 30–50 μL of SOPC solution with concentration of 1 g/L in chloroform-methanol (9:1 volume parts) on the ITO side of each ITO-coated glass plate. Subsequently, the electrodes were held for at least 2 hr under vacuum until the lipid completely dried, whereafter, the electroformation chamber was assembled to completely fill the internal volume with 0.2 M solution of sucrose. Then an alternating electric field with frequency of 10 Hz and peak-to-peak amplitude, successively increased up to 0.3 V/mm, was applied. In approximately 2 hr, a high yield of unilamellar vesicles with radii of tens of micrometers was obtained and taken out of the electroformation chamber. After the addition of the appropriate glucose solution to the vesicular suspension, we proceeded to the electrodeformation experiment as described further.

B. Experimental setup and measurements

Until now, the experimental equipments for GUV electrodeformation have used AC sinusoidal signals [21–23] or short DC pulses [26–30]. Both of them have been applied by internal electrodes (in direct contact with the vesicular suspension). To avoid electrochemical degradation of the sample, these investigations have been limited only to fast processes in the membrane, like electro-polarization and electroporation. In the experiments presented here we used a specially designed sample container allowing the application of moderate to strong AC fields with low frequency (a few kHz). The holder geometry has been already used for electro-optical studies of aqueous colloidal suspensions [31] and is described in detail elsewhere [32].

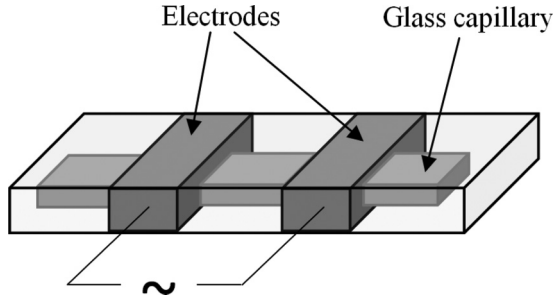


FIG. 1. Schematic presentation of the experimental setup for electrodeformation of GUVs consisting of a flat optical capillary ($200\ \mu\text{m}$ -thick walls at a distance $d = 200\ \mu\text{m}$) and a pair of aluminum electrodes, placed directly on the outside of the capillary glass wall; the distance between the electrodes is $l = 2\ \text{mm}$.

Thin flat optical capillaries (VetroCom, NJ) with internal cross section $0.2 \times 2.0\ \text{mm}^2$ were used as sample containers. Prior to electrodeformation experiment, a capillary was filled with GUV suspension and flame sealed to avoid evaporation. The electric field was applied by external electrodes made of a couple of aluminum foil rings wrapped around the capillary at a distance $l = 2\ \text{mm}$ (see Fig. 1).

The chosen construction permitted the capillary to be freely translated inside the aluminum rings in order to extend the observed region from the sample during the experiment. The applied sinusoidal AC voltage with variable amplitude and frequency was generated by a TGA1241 generator and amplified ($\times 200$) by a high-voltage amplifier TREK 2220.

For the setup described above the electric field penetration in the capillary is affected by the capillary glass walls. The effective (root mean square) value E of the field inside the suspension can be written as [32]

$$E = c_d(f)c_s(f)U_{\text{eff}}/l, \quad (1)$$

where the coefficients $c_d(f)$ and $c_s(f)$ are frequency-dependent correction factors accounting for the field attenuation in the sample as described in detail elsewhere [32]. The factor $c_d(f)$ arises because of the different dielectric properties of the glass and the suspension. The factor $c_s(f)$ is due to the field screening by the mobile charges, accumulated on the wall-suspension interface when the frequency is lower than the charge relaxation frequency $f_c = K/(2\pi\epsilon_0\epsilon_s)$ of the suspension. Here K and ϵ_s denote the conductivity and the dielectric constant of the suspension, respectively. Moreover, the correction coefficients $c_s(f)$ and $c_d(f)$ depend on the geometry of the external electrodes. For a simple sandwich-cell geometry they can be calculated analytically [33,34]. In our case (see Fig. 1), where the field is directed along the glass-liquid interface, the correction coefficients were determined numerically [35].

As far as the vesicle tubulation reported here was observed only in the prolate case, we performed all the experiments at two field frequencies of 1 kHz or 2 kHz at which vesicles assumed prolate ellipsoid shapes. The use of these field frequencies provided the best compromise between the low field penetration in the sample (no more than a few percent) [32] and the maximum voltage accessible with our apparatus $U = 2\ \text{kV}$. An important benefit of the applied

electrode geometry is the relatively long time (several minutes) of the field application, which permitted the visualization and the registration of the vesicle electrodeformation using an Olympus BX51-P microscope (Japan) and AM7023CT digital camera (Dino-Lite, France).

III. RESULTS AND DISCUSSION

We observed and registered AC field-induced tubulation from membranes of GUVs. To the best of our knowledge, such a phenomenon has not been previously reported in the literature.

The pictures of tether formation and its evolution with variation of the electric field amplitude are presented in Fig. 2. A sinusoidal AC signal with frequency $f = 2\ \text{kHz}$ and amplitudes up to $500\ \text{V}$ was applied to the external electrodes for several minutes (Fig. 1). Under the application of the electric field the vesicle assumed a prolate ellipsoid shape with its long axis toward the field. This prolate shape [Fig. 2(b)] was observed at $U = 300\ \text{V}$. The increasing of the voltage to approximately $350\ \text{V}$ led to the occurrence of an unstable lemon-like shape followed by the fast formation of two opposite tubular protrusions along the field direction [Fig. 2(c)]. At $500\ \text{V}$ they were already pulled out at a length of hundreds of micrometers out of the vesicle [in Fig. 2(d) the tether ends beyond the picture frames].

The evolution of the tether length with increasing the field amplitude is presented in Fig. 3. Three data sets are shown corresponding to three different vesicle radii ($8\ \mu\text{m}$, $23.5\ \mu\text{m}$, and $25\ \mu\text{m}$) and two field frequencies: $f_1 = 1\ \text{kHz}$ and $f_2 = 2\ \text{kHz}$. The experimental data provided evidence for the threshold character of the field-strength effect on the length of the observed membrane protrusions. The frequency dependence (if any) of the threshold field could be a subject of future experiments.

The radii of the tubular protrusions r were found to be almost independent of the vesicle size (Fig. 4). We measured the tube diameters by performing image analysis of the light intensity profile along a straight line perpendicular to the tube

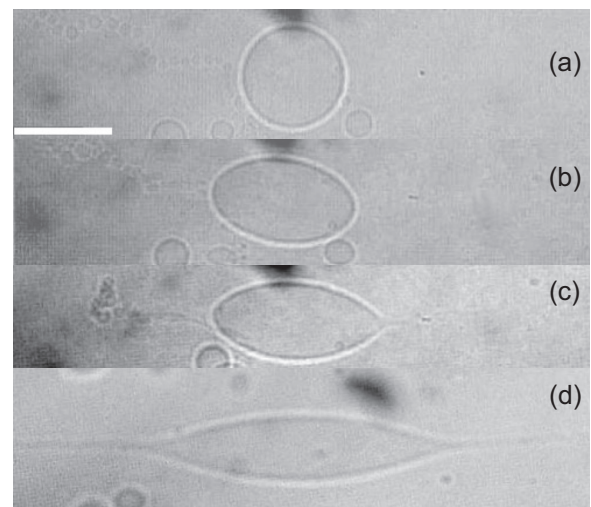


FIG. 2. Vesicle morphology under AC voltage of different amplitude U at $f = 2\ \text{kHz}$: (a) $U = 0\ \text{V}$; (b) $U = 300\ \text{V}$; (c) $U = 350\ \text{V}$; (d) $U = 500\ \text{V}$. The bar corresponds to $50\ \mu\text{m}$.

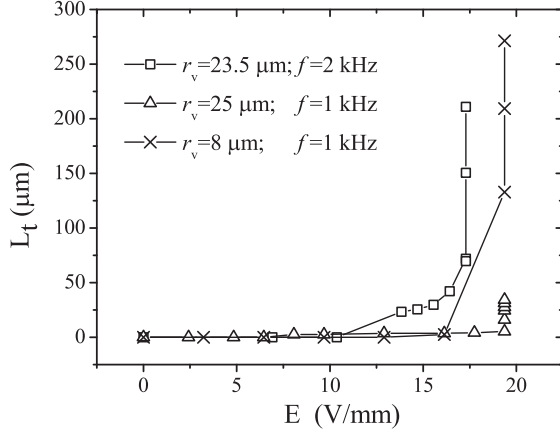


FIG. 3. Dependence of the tether length on the electric field strength for three vesicle radii.

axis with accuracy limited by the spatial resolution of our optical system ($0.52 \mu\text{m}/\text{pix}$). The average tube radius $r = 2.3 \pm 0.2 \mu\text{m}$ was determined as the weighed mean value of the data acquired from nine vesicles. It is noteworthy that in our experiment the vesicles were freely floating in the suspension, while in previous studies, discussing the dependence of the tether radius on optical tweezers dragging force, the vesicles have been held at constant membrane tension [36,37]

As far as in our experiment we applied low-frequency electric fields, the transmembrane potential U_{tm} arising from the accumulation of countercharges on both sides of the vesicle membrane can be estimated using [27,30,38]

$$U_{tm}(t) = 1.5R(\mathbf{E} \cdot \mathbf{n})[1 - \exp(-t/\tau)], \quad (2)$$

where R is the vesicle radius, \mathbf{n} is the normal to the lipid bilayer, and τ is the characteristic time for charge accumulation (here $\tau \ll t$). This potential is sustained by the membrane and reaches its maximum at both vesicle poles facing the electrodes ($\mathbf{E} \parallel \mathbf{n}$). The transmembrane potential is related to an electro-induced surface tension of the membrane σ_{el} expressed by [39–42]

$$\sigma_{el} \approx \varepsilon_0 \varepsilon_m U_{tm}^2 / (2h_m), \quad (3)$$

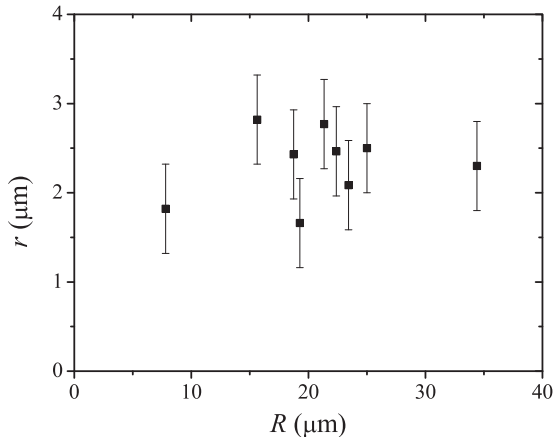


FIG. 4. Experimental data for the tube radius r and the corresponding vesicle radius R . The error bars are determined from the optical resolution of the system ($0.52 \mu\text{m}/\text{pixel}$)

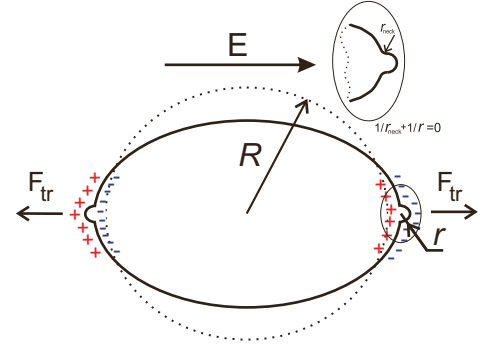


FIG. 5. Pulling tubular protrusions from a vesicle in alternating electric field. Dotted line denotes the initial quasispherical shape of the vesicle (at $E = 0$). The inset shows the cap's neck with its zero total curvature.

where ε_0 is the dielectric permittivity of the vacuum, ε_m is the relative dielectric permittivity for the membrane, and h_m is the total bilayer thickness. The surface tension term σ_{el} results from the compressive electric stress created by the electrostatic attraction between the ions accumulated on the two sides of the impermeable lipid bilayer (for a review on the dynamics of giant vesicles in electric fields, see Ref. [42]).

The proposed mechanism of tube formation is represented in Fig. 5. We assume that as a result of the counterions migration the tube elongation is started with the formation of membrane caps at the vesicle poles facing the electrodes. Taking into account that the membrane tethers are pulled along the electric field direction and $\mathbf{E} \perp \mathbf{n}$ the transmembrane potential on the cylindrically bent bilayer of the tether is zero [(see Eq. (2)]. Therefore, the tensile electric force acting on the tether caps F_{tr} and triggering the tether formation is given by [43,44]

$$F_{tr} = 2\pi\sqrt{2k_c\sigma}, \quad (4)$$

where k_c is the bending elasticity modulus and σ is the membrane tension.

In what follows we evaluate the transmembrane potential σ_{el} and the triggering pulling force F_{tr} from our experiment. The penetrated electric field into the sample $E = 17.3 \text{ V/mm}$ was obtained from Eq. (1). Using the experimental value of the tube radius, $r = 2.3 \mu\text{m}$, we determined the transmembrane potential on the membrane caps $U_{tm} = 0.06 \text{ V}$ from Eq. (2). From Eq. (3) we evaluated the electrically induced membrane tension $\sigma_{el} = 9 \mu\text{N/m}$ using the values for SOPC bilayer thickness $h_m = 3.9 \text{ nm}$ [45] and its relative dielectric permittivity $\varepsilon_m = 2.2$ [46]. The transmembrane potential U_{tm} and the membrane tension σ_{el} obtained here are below the critical values reported for membrane electroporation, namely, $U_{cr} \approx 1 \text{ V}$ [27] and $\sigma_{cr} \approx 6 \text{ mN/m}$ [39]. Then we can estimate the triggering pulling force using Eq. (4) and the bending modulus of SOPC membranes $k_c \sim 2 \times 10^{-19} \text{ J}$ [47]. It reads $F_{tr} = \sim 12 \text{ pN}$. In the case of nanotube formation, the corresponding optical tweezers dragging force was reported in the range of $0.6 < F_{tr} < 20 \text{ pN}$ [36,44,48,49].

The protrusion formation is accompanied by a relative motion between the monolayers comprising a 10-fold increase in curvature bilayer near the vesicle-tether junction

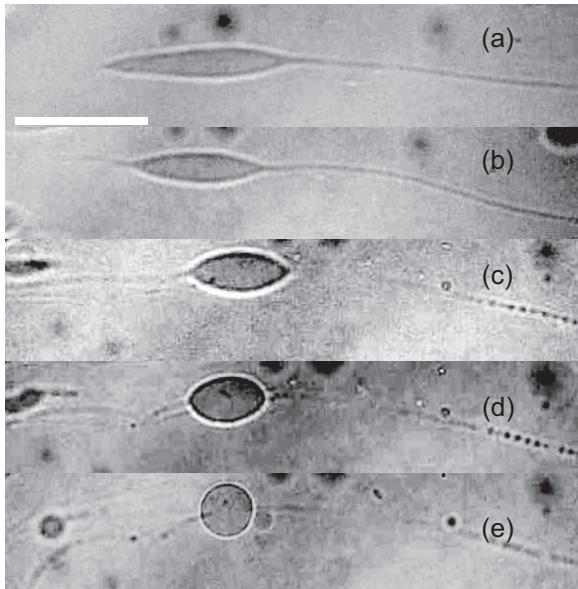


FIG. 6. (a) Vesicle morphology under AC voltage of amplitude $U = 1200$ V and $f = 1$ kHz. Relaxation after switching off the field ($U = 0$ V): (b) 1 s; (c) 5 s; (d) 10 s; (e) 20 s. The bar corresponds to $50 \mu\text{m}$.

($r \sim 2 \mu\text{m}$, $R \sim 20 \mu\text{m}$). The energy dissipation arising from the viscous effect of the slipping retardation in the lipid monolayers accompanying the tube formation must be taken into account [50,51]. The radii during the elongation remained constant, and the viscoelastic force is characterized by a single effective viscosity η_{eff} including the surface membrane viscosity and the intermonolayer slip coefficient [48]. The viscoelastic force is given by $F_v = 2\pi\eta_{\text{eff}}V_t$, where V_t is the rate of the tether elongation. For SOPC at room temperature the effective viscosity has been reported as $\eta_{\text{eff}} = 0.009$ pN s/m [50] and $V_t \approx 50 \mu\text{m/s}$ was determined from our experiment, thus obtaining the viscoelastic force: $F_v \sim 3$ pN. The estimated pulling force is balancing the viscous dissipation due to the intermonolayer slipping thus leading to the observed stationary elongation of protrusions.

At small voltages (lower than 300 V) no tubular protrusions appeared and the vesicle fully recovered its quasispherical shape at $U = 0$ V. At higher applied voltages, after the formation of membrane tubes [see Fig. 6(a)] and switching

off the electric field, the following relaxation of the vesicle is shown in Figs. 6(b)–6(e). As illustrated there, the tube relaxation exhibited a stable pearling phase. Our observations suggest that no electroporation effects occurred during the application of the electric field thus vesicle images remaining well contrasted throughout all the experiment. The appearance of similar pearling instability has been reported in Ref. [52] for cylindrical vesicles in AC fields with frequencies one order of magnitude higher than here. In our experiment the pearling phase remained stable with time (for tens of minutes) after the electric field was turned off. As pointed out above, neutral lipid membranes in electric fields are expected to reduce their surface tension due to the electrostatic interaction between the free charges accumulated on the two sides of the bilayer from the conductive water solution [41]. Correspondingly, the pearling morphological change in the tethers observed here testifies to an increase of the membrane surface tension when the electric field was switched off. Our observation is coherent with experimental findings published in the literature about a decrease in the surface tension of lipid bilayers in electric fields [53,54].

IV. CONCLUSIONS

We reported on the formation of tubular membrane protrusions from giant unilamellar vesicles in the presence of alternating electric field. Our experimental setup made possible the application of strong AC electric field with low frequency (\sim kHz) for a relatively long time period (minutes) permitting the *in situ* control of the electro-induced vesicle morphology. The size of the tubes was in the micrometer scale and was found to be independent of the vesicle radius. The registered tube formation was related to a threshold electric field estimated to be below the field strengths inducing membrane electroporation.

ACKNOWLEDGMENTS

We thank professors I. Dozov and G. Popkirov for the stimulating discussions. The work is related to the COST Action TD1104 European Network for Development of Electroporation-Based Technologies and Treatments (EP4Bio2Med), www.electroporation.net. V.V. acknowledges support from the National Science Fund at the Ministry of Education and Science (Bulgaria), Grant No. DMU03-80/2011.

-
- [1] C. Lee and L. B. Chen, *Cell* **54**, 37 (1988).
 - [2] K. Hirschberg, Ch. M. Miller, J. Ellenberg, J. F. Presley, E. D. Siggia, R. D. Phair, and J. Lippincott-Schwartz, *J. Cell Biol.* **143**, 1485 (1998).
 - [3] M. P. Sheetz, *Nat. Rev. Mol. Cell. Biol.* **2**, 392 (2001).
 - [4] W. Römer, L. Berland, V. Chambon, K. Gaus, B. Windschieg, D. Tenza, M. R. E. Aly, V. Fraisier, J.-C. Florent, D. Perrais, C. Lamaze, G. Raposo, C. Steinem, P. Sens, P. Bassereau, and L. Johannes, *Nature (London)* **450**, 670 (2007).
 - [5] D. Acehan, A. Malhotra, Y. Xu, M. Ren, D. L. Stokes, and M. Schlame, *Biophys. J.* **100**, 2184 (2011).
 - [6] A. V. Shnyrova, V. A. Frolov, and J. Zimmerberg, *Curr. Biol.* **19**, R772 (2009).
 - [7] J. C. Stachowiak, C. C. Hayden, and D. Y. Sasaki, *Proc. Natl. Acad. Sci. USA* **107**, 7781 (2010).
 - [8] B. Sorre, A. Callan-Jones, J. Manzi, B. Goud, J. Prost, P. Bassereau, and A. Roux, *Proc. Natl. Acad. Sci. USA* **109**, 173 (2012).
 - [9] R. C. Sarasij, S. Mayor, and M. Rao, *Biophys. J.* **92**, 3140 (2007).
 - [10] Y. Yamashita, S. M. Masum, T. Tanaka, Y. Tamba, and M. Yamazaki, *Langmuir* **18**, 9638 (2002).

- [11] I. Tsafirir, Y. Caspi, M.-A. Guedeau-Boudeville, T. Arzi, and J. Stavans, *Phys. Rev. Lett.* **91**, 138102 (2003).
- [12] V. Kralj-Iglič, H. Hägerstrand, P. Veranič, K. Jezernik, B. Babnik, D. R. Gauger, and A. Iglič, *Eur. Biophys. J.* **34**, 1066 (2005).
- [13] J. Varkey, J. M. Isas, N. Mizuno, M. B. Jensen, V. K. Bhatia, C. C. Jao, J. Petrova, J. Voss, D. Stamou, A. C. Steven, and R. Langen, *J. Biol. Chem.* **285**, 32486 (2010).
- [14] Y. Li, R. Lipowsky, and R. Dimova, *Proc. Natl. Acad. Sci. USA* **108**, 4731 (2011).
- [15] A.-F. Bitbol, N. Puff, Y. Sakuma, M. Imai, J.-B. Fournier, and M. I. Angelova, *Soft Matter* **8**, 6073 (2012).
- [16] C. Martin, S. F. Pedersen, A. Schwab, and C. Stock, *Am. J. Physiol.-Cell Physiol.* **300**, C490 (2011).
- [17] M. Winterhalter and W. Helfrich, *J. Colloid Interface Sci.* **122**, 583 (1988).
- [18] M. D. Mitov, P. Meleard, M. Winterhalter, M. I. Angelova, and P. Bothorel, *Phys. Rev. E* **48**, 628 (1993).
- [19] K. A. Riske and R. Dimova, *Biophys. J.* **88**, 1143 (2005).
- [20] R. Dimova, K. A. Riske, S. Aranda, N. Bezlyepkina, R. L. Knorr, and R. Lipowsky, *Soft Matter* **3**, 817 (2007).
- [21] S. Aranda, K. A. Riske, R. Lipowsky, and R. Dimova, *Biophys. J.* **95**, L19 (2008).
- [22] K. Antonova, V. Vitkova, and M. D. Mitov, *Europhys. Lett.* **89**, 38004 (2010).
- [23] P. Peterlin, *J. Biol. Phys.* **36**, 339 (2010).
- [24] M. Angelova and D. S. Dimitrov, *Progr. Colloid Polymer Sci.* **76**, 59 (1988).
- [25] V. Vitkova, K. Antonova, G. Popkirov, M. D. Mitov, Yu. A. Ermakov, and I. Bivas, *J. Phys.: Conf. Ser.* **253**, 012059 (2010).
- [26] T. Portet and R. Dimova, *Biophys. J.* **99**, 3264 (2010).
- [27] U. Zimmermann, *Biochim. Biophys. Acta* **694**, 227 (1982).
- [28] R. S. Gracia, N. Bezlyepkina, R. L. Knorr, R. Lipowsky, and R. Dimova, *Soft Matter* **6**, 1472 (2010).
- [29] P. F. Salipante, R. L. Knorr, R. Dimova, and P. Vlahovska, *Soft Matter* **8**, 3810 (2012).
- [30] K. Kinoshita Jr., I. Ashikawa, N. Saita, and H. Yoshimura, *Biophys. J.* **53**, 1015 (1988).
- [31] E. Paineau, K. Antonova, C. Baravian, I. Bihannic, P. Davidson, I. Dozov, M. Imperor-Clerc, P. Levitz, A. Madsen, F. Meneau, and L. J. Michot, *J. Phys. Chem. B* **113**, 15858 (2009).
- [32] K. Antonova, I. Dozov, P. Davidson, E. Paineau, C. Baravian, I. Bihannic, and L. J. Michot, *Bulg. J. Phys.* **39**, 72 (2012).
- [33] L. D. Landau and E. M. Lifshitz, *Electrodynamics of Continuous Media* (Pergamon Press, Oxford, 1960).
- [34] A. F. Demirörs, P. M. Johnson, C. M. van Kats, A. van Blaaderen, and A. Imhof, *Langmuir* **26**, 14466 (2010).
- [35] I. Dozov, E. Paineau, P. Davidson, K. Antonova, C. Baravian, I. Bihannic, and L. J. Michot, *J. Phys. Chem. B* **115**, 7751 (2011).
- [36] T. Roopa, N. Kumar, S. Bhattacharya, and G. V. Shivashankar, *Biophys. J.* **87**, 974 (2004).
- [37] R. M. Hochmuth and E. A. Evans, *Biophys. J.* **39**, 71 (1982).
- [38] W. Harbich, W. Helfrich, *Z. Naturforsch.* **34**, 1063 (1979).
- [39] D. Needham and R. M. Hochmuth, *Biophys. J.* **55**, 1001 (1989).
- [40] I. G. Abidor, V. B. Arakelyan, L. V. Chernomordik, Y. A. Chizmadzhev, V. F. Pastushenko, and M. R. Tarasevich, *J. Electroanal. Chem.* **104**, 37 (1979).
- [41] P. M. Vlahovska, R. S. Gracia, S. Aranda-Espinoza, and R. Dimova, *Biophys. J.* **96**, 4789 (2009).
- [42] P. Vlahovska, *Soft Matter* **11**, 7232 (2015).
- [43] V. Heinrich and R. E. Waugh, *Ann. Biomed. Eng.* **24**, 595 (1996).
- [44] D. Cuvelier, N. Chiaruttini, P. Bassereau, and P. Nassoy, *Europhys. Lett.* **71**, 1015 (2005).
- [45] P. R. Rand, N. Fuller, V. A. Parsegian, and D. C. Rau, *Biochemistry* **27**, 7711 (1988).
- [46] R. Fettiplace, D. M. Andrews, and D. A. Maydon, *J. Membr. Biol.* **5**, 277 (1971).
- [47] J. Genova, V. Vitkova, and I. Bivas, *Phys. Rev. E* **88**, 022707 (2013).
- [48] R. M. Hochmuth, Jin-Yu Shao, J. Dai, and M. P. Sheetz, *Biophys. J.* **70**, 358 (1996).
- [49] T. Inaba, A. Ishijima, M. Honda, F. Nomura, K. Takiguchi, and H. Hotani, *J. Mol. Biol.* **348**, 325 (2005).
- [50] E. Evans and A. Yeung, *Chem. Phys. Lipids* **73**, 39 (1994).
- [51] I. Bivas, P. Meleard, I. Mircheva, and P. Bothorel, *Coll. Surf. A: Physicochem. Eng. Asp.* **157**, 21 (1999).
- [52] K. P. Sinha, S. Gadkari, and R. M. Thakkar, *Soft Matter* **9**, 7274 (2013).
- [53] S. Lecuyer, G. Fragneto, and T. Charitat, *Eur. Phys. J. E: Soft Matter Biol. Phys.* **21**, 153 (2006).
- [54] T. Charitat, S. Lecuyer, and G. Fragneto, *Biointerphases* **3**, FB3 (2008).